Dynamics of the three-dimensional expansion in a vapor produced by a laser pulse

S. I. Anisimov, B. S. Luk'yanchuk, and A. Luches

L. D. Landau Institute of Theoretical Physics, Russian Academy of Sciences, Chernogolovka,
142 432 Moscow Region, Russia

Studies are reported of the expansion into vacuum of a cloud of dense vapor produced by the action of a nanosecond laser pulse on the surface of a solid body. The investigation is based on the well-known particular solution of the gasdynamic equations describing the expansion into vacuum of a gas cloud in the shape of a triaxial ellipsoid. The analysis presented here provides an explanation for the "flipover" effect observed in a deposited spot. It is shown that the solution thus constructed can be used to interpret the results of time-of-flight mass spectroscopy and to describe the shape of a vapor cloud expanding into a medium with an ambient pressure. The rate of flow of vapor onto a planar substrate and the transverse profile of the film that forms as a result of vapor condensation on the substrate are calculated. The dependence of this profile on the shape of the focal spot is determined. A simple analytical expression is found for the transverse profile in the range of parameters typical of the laser technique for obtaining thin films. © *1995 American Institute of Physics.*

1. INTRODUCTION

In recent years vaporization by pulsed laser radiation has come into wide use for depositing thin films. This technique is used to obtain and process films of high-temperature superconducting materials, multilayer metal mirrors for x-ray radiation, diamondlike carbon films, etc. (see the reviews in Refs. 1–6). The deposited films are nonuniform in thickness. The profile of the film thickness is determined by the angular distribution of the flux of vaporized material, which depends in turn on the vaporization regime and the shape of the focal spot. The angular distribution of laser ablation products has been studied in considerable detail both experimentally and theoretically (see, e.g., Refs. 7–18). However, in almost all theoretical treatments the expansion of the vapor has been assumed to be isothermal, which is inconsistent with both experiment[19–21] and with numerical simulations (see, e.g., Ref. 22). Previously[17] we have considered the case of adiabatic vapor expansion. However, the analysis in Ref. 17 applies to the special case of axisymmetric vapor flow, which is obtained when the focal spot has a circular shape. Experiments and applications frequently use beams with noncircular aperture which are obliquely incident on the target. Under these conditions the vapor flow is nonaxisymmetric. It should be noted that the cloud does not "forget" the initial asymmetry as it expands. On the contrary, the shape of the cloud in the late stages of expansion and the profile of the deposited film are determined by precisely this initial asymmetry. Experiments[9,12,13] reveal, e.g., that in the case of an elliptical focal spot the deposited material forms a spot on the substrate which is also of elliptical shape, but with axes rotated through 90° (the so-called flipover effect). Such effects can naturally not be explained if we restrict ourselves to treating axisymmetric flows.

Note that the spatial structure of a vapor (plasma) formed on the surface of a solid target under the action of a nanosecond laser pulse was studied experimentally in detail as early as the 1960s. It was established (see, e.g., Ref. 19)

that a dense cloud ($n \geq 10^{21}$ cm^{-3}) of vaporized material develops right at the surface of the target, and that its size increases in the course of the laser pulse. This increase in the dimension is due mainly to evaporation of the target material. It is sharply reduced after the end of the pulse. Then the observed boundary of the dense cloud begins to slowly shift back toward the surface because of expansion of the cloud into vacuum. This process of the expansion of the dense cloud will also be studied in the present work. Because the density of the evaporated material is high we will describe the expansion process using the gasdynamic equations, as is done in the majority of treatments of vaporization by laser pulses. A simple estimate shows that in typical cases this approximation remains fairly accurate as long as the size of the cloud is less than 3–10 cm. If the radiation intensity is sufficiently high the dense cloud is surrounded by a tenuous plasma envelope, the outer layer of which consists of electrons and the inner of ions. Because its mass is relatively low this plasma envelope has essentially no influence on the expansion dynamics of the dense core.

The study of the three-dimensional dynamics of the gas flare presented below is based on the well-known particular solution of the gasdynamic equations describing flows with uniform deformation. This particular solution exists by virtue of the invariance of the gasdynamic equations with respect to a certain Lie group (for more detail see Refs. 23 and 24). One-dimensional flows of this type (with flow velocity proportional to the distance from the center of symmetry) were first studied by Sedov.[25] Ovsyannikov[26] considered the general three-dimensional case and showed that for flows with uniform deformation the gasdynamic equations can be reduced to a system of ordinary differential equations describing the dynamics of a point in a nine-dimensional space. This same result was later derived by Dyson.[27] The system of equations derived in Refs. 26 and 27 has been integrated numerically,[17,27–29] or analytically[30] in a number of special
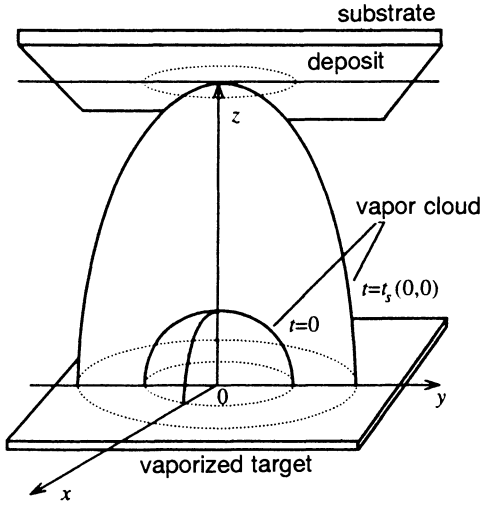
FIG. 1. Schematic of an experiment for laser deposition of films.

cases. Bogoyavlenski[31] carried out a qualitative investigation of this system of equations.

Particular solutions of this class can be constructed for an arbitrary initial temperature profile. In recent years simple solutions of the form given in Ref. 26 with constant temperature have been used frequently to analyze experimental data on laser ablation (see, e.g., Refs. 10, 11, and 14). The authors of these treatments, in all probability, are unfamiliar with the more general results derived in Refs. 23–31, and they restricted themselves to the approximation of isothermal flow, which, as was noted above, does not entirely agree with the experimental situation. The physical inadequacy of the isothermal solution (there is no mechanism in gasdynamics that would maintain a finite temperature at the boundary of the vapor cloud) is well known and has been discussed in detail, e.g., in Ref. 24. Since in the present work we are interested mainly in the motion of the vapor after the conclusion of the laser pulse, it seems closer to reality and physically more correct to assume that the vapor flow is isentropic, as was done in Ref. 17. In the present work we will follow the formulation of the problem used in Ref. 17.

We will treat the adiabatic expansion of a one-component vapor cloud into vacuum. A schematic of the experiment is shown in Fig. 1. We will assume that the time for the formation of the vapor cloud at the target surface (which is close to the duration of the laser pulse) is much less than its expansion time, which is determined by the distance between the target and the substrate on which the vaporized material condenses. For this reason the expansion of the vapor cloud into vacuum can be treated independently of the formation process. We will assume that the focal spot has an elliptical shape with semiaxes X_0 and Y_0. The expansion of the cloud of vaporized material will be modeled by the expansion of a triaxial gaseous ellipsoid whose semiaxes are initially equal to X_0, Y_0, and $Z_0 \approx c_s t_0$, where t_0 is the duration of the laser pulse and c_s is the speed of sound in the vaporized material. In this formulation the problem of the three-dimensional expansion of the vapor cloud admits a relatively simple solution, and the profile of the film thickness can be described by a simple analytical formula.

2. MODEL

Consider the adiabatic expansion into vacuum of a gas cloud in the shape of an ellipsoid with semiaxes X_0, Y_0, and Z_0. The expansion is described by the equations of gasdynamics

$$\frac{\partial \rho}{\partial t} + \mathrm{div}(\rho, \mathbf{v}) = 0, \tag{1}$$

$$\frac{\partial \mathbf{v}}{\partial t} + (\mathbf{v}\nabla)\mathbf{v} + \frac{1}{\rho}\nabla p = 0, \tag{2}$$

$$\frac{\partial S}{\partial t} + \mathbf{v}\nabla S = 0, \tag{3}$$

where ρ, p, $\mathbf{v}$, and S are respectively the density, pressure, velocity vector, and entropy of the gas. We will describe the vaporized material using the ideal-gas equation of state with a constant adiabatic index $\gamma = c_p / c_V$. In this case Eq. (3) for the entropy in the system (1)–(3) can be transformed into an equation for the pressure p:

$$\frac{\partial p}{\partial t} + \mathbf{v}\nabla p + \gamma p \ \mathrm{div}\ \mathbf{v} = 0. \tag{4}$$

A particular solution describing the expansion of an ellipsoid can be written in the form[26]

$$r_i(t) = F_{ik}(t)r_k(0), \quad i = x,y,z. \tag{5}$$

Here $r_i(t)$ are the Eulerian coordinates of a gas particle and $r_k(0)$ are its Lagrangian coordinates. Summation is implied by repeated indices. The diagonal elements of the matrix F_{ik} describe the change in volume of the cloud and the off-diagonal elements describe its rotation. Neglecting rotation we can write the matrix F_{ik} in the form

$$F_{ik} = \begin{vmatrix} X(t)/X_0 & 0 & 0 \\ 0 & Y(t)/Y_0 & 0 \\ 0 & 0 & Z(t)/Z_0 \end{vmatrix}, \tag{6}$$

where X_0, Y_0, and Z_0 are the initial values of $X(t)$, $Y(t)$, and $Z(t)$. From (5) it follows immediately that the mass velocity of a gas particle depends linearly on its radius vector,

$$v_i = \dot{F}_{ik}F_{kj}^{-1}r_j, \tag{7}$$

where F^{-1} is the reciprocal of the matrix F and the dot is used to indicate differentiation with respect to time. It can be shown (see, e.g., Ref. 31) that for adiabatic motions of a gas of the form (5) the gasdynamic system of equations (1)–(3) reduces to a system of ordinary differential equations if the pressure and density of the gas have the form

$$p(\mathbf{r},t) = h(t)H(\chi), \quad \rho(\mathbf{r},t) = f(t)\frac{dH}{d\chi},$$

$$\chi = g_{ik}r_i(0)r_k(0),$$

$$f(t) = A[\det(F_{ik})]^{-1}, \quad h(t) = B[\det(F_{ik})]^{-\gamma}, \tag{8}$$

where A and B are constants and g_{ik} is a constant symmetric matrix. For a matrix F_{ik} of the form (6) the pressure and density profiles can be written as follows:

$$p(\mathbf{r},t) = \frac{E}{I_2(\gamma)XYZ}\left[\frac{X_0Y_0Z_0}{XYZ}\right]^{\gamma-1}$$
$$\times\left[1 - \frac{x^2}{X^2} - \frac{y^2}{Y^2} - \frac{z^2}{Z^2}\right]^{\gamma/\gamma-1}, \tag{9}$$

$$\rho(\mathbf{r},t) = \frac{M}{I_1(\gamma)XYZ}\left[1 - \frac{x^2}{X^2} - \frac{y^2}{Y^2} - \frac{z^2}{Z^2}\right]^{1/\gamma-1}. \tag{10}$$

Here $M = \int \rho(\mathbf{r},t)dV$ is the total mass and $E = (\gamma-1)^{-1}\int p(\mathbf{r},0)dV$ is the initial energy of the vaporized material. The normalization constants I_1 and I_2 appearing in Eqs. (9) and (10) are equal to

$$I_1(\gamma) = \pi\Gamma\left[\frac{\gamma}{\gamma-1}\right]\Gamma\left[\frac{3}{2}\right]/\Gamma\left[\frac{\gamma}{\gamma-1}+\frac{3}{2}\right],$$

$$I_2(\gamma) = \frac{\pi}{\gamma-1}\Gamma\left[\frac{\gamma}{\gamma-1}+1\right]\Gamma\left[\frac{3}{2}\right]/\Gamma\left[\frac{\gamma}{\gamma-1}+\frac{5}{2}\right],$$

where $\Gamma(z)$ is the gamma function.

After substituting (5), (9), and (10) into the gasdynamic equations (1)–(3) we arrive at a system of ordinary differential equations for the matrix elements $X(t)$, $Y(t)$, and $Z(t)$. These can be written in the form of equations of motion of a point mass in classical mechanics:

$$\ddot{X} = -\frac{\partial U}{\partial X}, \quad \ddot{Y} = -\frac{\partial U}{\partial Y}, \quad \ddot{Z} = -\frac{\partial U}{\partial Z}, \tag{11}$$

where

$$U = \frac{(5\gamma-3)}{(\gamma-1)}\frac{E}{M}\left[\frac{X_0Y_0Z_0}{XYZ}\right]^{\gamma-1}. \tag{12}$$

The initial conditions for Eqs. (11) can be written in the form

$$X|_{t=0} = X_0, \quad Y|_{t=0} = Y_0, \quad Z|_{t=0} = Z_0,$$
$$\dot{X}|_{t=0} = 0, \quad \dot{Y}|_{t=0} = 0, \quad \dot{Z}|_{t=0} = 0. \tag{13}$$

In (13) we have assumed that the initial kinetic energy of the vapor is much less than its thermal energy.

In the general case Eq. (11) must be solved numerically. Examples of the numerical integration of such equations can be found in Refs. 10, 14, 17, and 27–29. In Ref. 30 it is shown that for $\gamma=5/3$ (in terms of the equations of mechanics this corresponds to a potential which is a homogeneous function of the coordinates of degree -2) the system (11) has an additional integral, which in the case of two degrees of freedom enables us to reduce the integration of Eqs. (11) to quadratures. This integral and the energy integral can be used to check the accuracy of a numerical calculation.

When we go over to the numerical integration of Eqs. (11) it is convenient to transform them somewhat. We choose the coordinate axes so that $X_0 \geqslant Y_0$ holds. In other words, we label the longest semiaxis of the initial gas ellipsoid with X_0. We introduce dimensionless variables, using X_0 as the length scale:

$$\xi = X/X_0, \quad \eta = Y/X_0, \quad \zeta = Z/X_0, \quad \tau = t\beta^{1/2}/X_0, \tag{14}$$

$$\eta_0 = Y_0/X_0, \quad \zeta_0 = Z_0/X_0, \quad \beta = (5\gamma-3)\frac{E}{M}.$$

The equations of motion (11) and initial conditions (13) are then transformed to

$$\xi\ddot{\xi} = \eta\ddot{\eta} = \zeta\ddot{\zeta} = \left[\frac{\eta_0\zeta_0}{\xi\eta\zeta}\right]^{\gamma-1},$$

$$\xi(0) = 1, \quad \eta(0) = \eta_0, \quad \zeta(0) = \zeta_0, \tag{15}$$

$$\dot{\xi}(0) = \dot{\eta}(0) = \dot{\zeta}(0) = 0.$$

In the variables (14) the energy integral takes the form

$$\frac{1}{2}(\dot{\xi} + \dot{\eta}^2 + \dot{\zeta}^2) + \frac{U(\tau)}{\beta} = \varepsilon = \text{const}, \tag{16}$$

where

$$\varepsilon = U(\tau=0)/\beta = (\gamma-1)^{-1}. \tag{17}$$

In the special case $\gamma=5/3$ Eqs. (15) have the additional constant of motion

$$\xi^2 + \eta^2 + \zeta^2 = 3\tau^2 + 1 + \eta_0^2 + \zeta_0^2. \tag{18}$$

3. NUMERICAL SOLUTION: THE FLIPOVER EFFECT

From (15) it is clear that the solution we are seeking depends on the three parameters γ, η_0, and ζ_0. The system of equations (15) was integrated numerically over the whole range of these parameters of interest for experiments on laser ablation. From Eqs. (15) it follows immediately that in the late stages of expansion the motion of the gas acquires an inertial character. In the limit $\tau\to\infty$ the ratios of the lengths of the axes of the ellipsoid which determines the cloud shape approach certain limiting values. These asymptotic values determine the angular dependence of the mass flux and the thickness profile of the film that forms. We introduce the variables $k_\eta(\tau) = \eta(\tau)/\xi(\tau)$ and $k_\zeta(\tau) = \zeta(\tau)/\xi(\tau)$, which determine the shape of the cloud at time τ. Examples of the functions $k_\eta(\tau)$ and $k_\zeta(\tau)$ for different values of γ, η_0, and ζ_0 are shown in Figs. 2 and 3 respectively.

The curves displayed in Fig. 2a correspond to different values of the adiabatic index γ for fixed η_0 and ζ_0. Note that for $\gamma<5/3$ the function $k_\eta(\tau)$ reaches its maximum at finite τ and then approaches its asymptotic value $k_\eta(\infty)$ from above. If we have $\gamma\geqslant5/3$ then $k_\eta(\tau)$ grows monotonically as a function of τ, and for τ of order 10^3 it reaches its limiting value $k_\eta(\infty)$. Figure 2b shows a family of $k_\eta(\tau)$ curves corresponding to different values of η_0 (the quantities γ and ζ_0 are held constant). For small τ the function $k_\eta(\tau)$ grows with time and for $\tau\approx10$ it reaches values $k_\eta=1$. At this point the expanding cloud becomes symmetric with respect to the z axis. Subsequently k_η continues to grow, i.e., the expansion proceeds more rapidly in the direction of the large initial pressure gradient (in the direction of the short axis). As a result, the deposited spot is rotated relative to the focal spot through an angle 90°. This is the explanation for the flipover effect mentioned above. Evidently this rotation effect should be observed for a focal spot of any shape having an axis of rotation of order n, C_n. The corresponding rotation angle is equal to π/n, i.e., the angle between the long and short sym-

FIG. 2. Time variation of the shape of the vapor cloud in the (x,y) plane (see text).
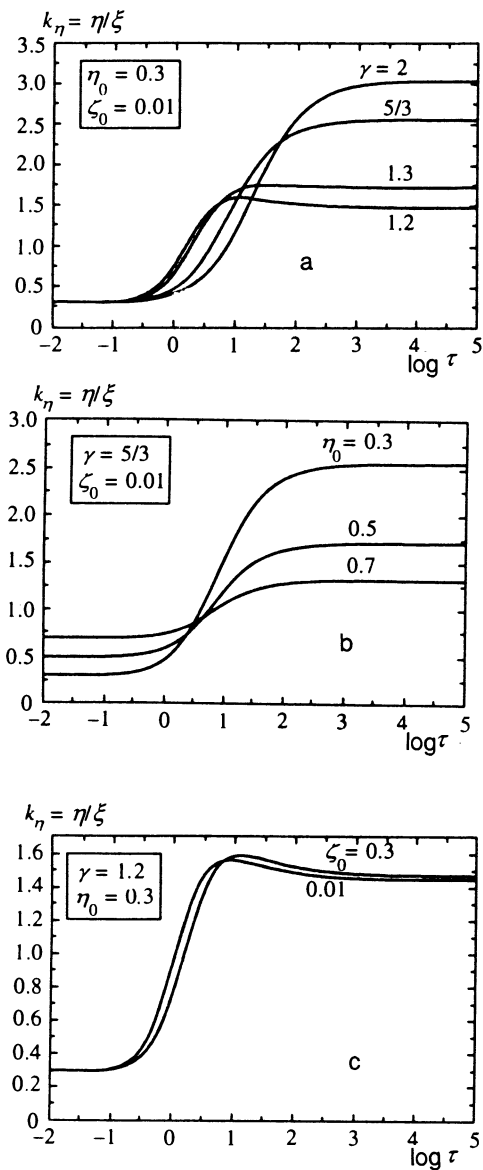

FIG. 3. Time variation of the shape of the vapor cloud in the (x,z) plane (see text).

metry axes of the figure. For a rectangle (as in the case of an ellipse) this angle is equal to 90°; for a regular triangle it is 60°; for a square it is 45°. Effects of this sort involving the rotation of a triangle and a square were recently observed in the condensation of vaporized material back on the original target in a medium with an ambient pressure.[18]

The family of curves in Fig. 2c illustrates the effect of the parameters ζ_0 on the nature of the cloud expansion in the (x,y) plane. It is clear that for the values η_0 and γ shown in the figure this effect is negligible: changing ζ_0 by a factor of 30 results in a change in k_η by a few percent. As γ increases and η_0 decreases the effect grows.

Figure 3 shows the function $k_\zeta(\tau)$ for different values of γ, η_0, and ζ_0. The behavior of k_ζ qualitatively resembles that of k_η. From Fig. 3a we see that the function $k_\zeta(\tau)$ is non-monotonic for $\gamma < 5/3$. Figure 3b shows the strong dependence of $k_\zeta(t)$ on the parameters ζ_0, while Fig. 3c shows that the dependence of $k_\zeta(t)$ on η_0 is weak. To summarize, we
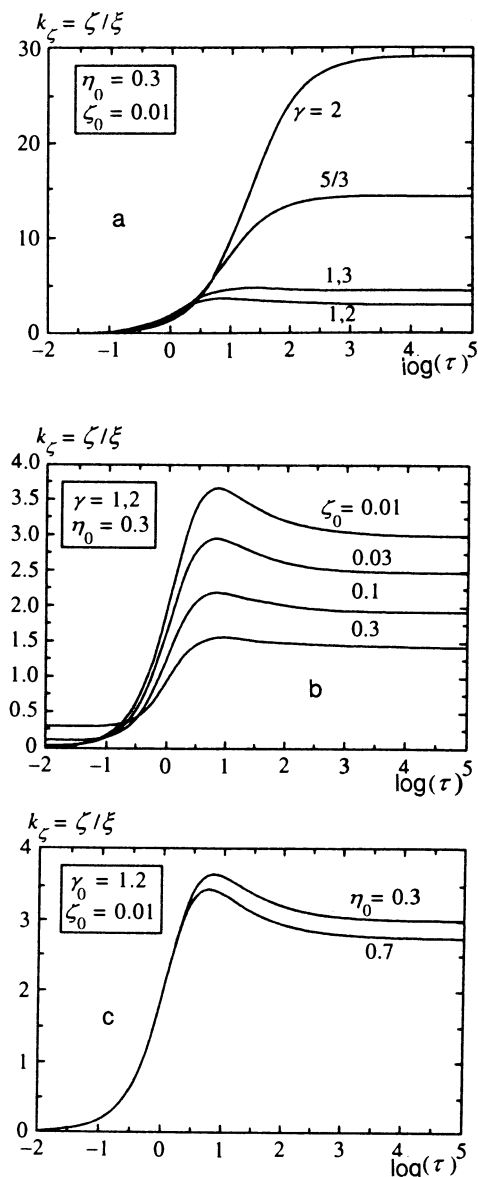
can say that the expansion of the cloud consists of a superposition of two weakly interacting motions. For a given adiabatic index γ the expansion of the cloud in the y direction is determined mainly by η_0 while expansion in the z direction is determined by ζ_0. If γ is not too close to unity, both motions become inertial for values of τ of order 100–1000. From then on the shape of the cloud remains practically unchanged, and the ratios of the lengths of the axes of the ellipsoid remain approximately equal to their asymptotic values $k_\zeta(\infty)$ and $k_\eta(\infty)$. Some of these values are given in Tables I and II. In these tables the columns and rows show the dependence on the variables for which the dependence is "strong": ζ_0 and γ for $k_\zeta(\infty)$, and η_0 and γ for $k_\eta(\infty)$. The column of three numbers in each box of the table illustrates the dependence on the least sensitive parameter: in Table I three values $k_\zeta(\eta_0=1)/k_\zeta(\eta_0=0.3)/k_\zeta(\eta_0=0.1)$ (reading downward) are given, while in Table II they are $2-k_\eta(\zeta_0=0.001)/k_\eta(\zeta_0=0.01)/k_\eta(\zeta_0=0.1)$. Note that

TABLE I.

$$k_\zeta = k_\zeta(\zeta_0, \gamma)$$

γ	ζ_0					
	0.001	0.003	0.01	0.03	0.1	0.3
1.1	2.16	1.97	1.77	1.59	1.39	1.20
	2.28	2.08	1.86	1.66	1.43	1.22
	2.40	2.18	1.93	1.71	1.45	1.22
1.2	3.69	3.18	2.67	2.24	1.79	1.39
	4.21	3.61	3.00	2.48	1.92	1.44
	4.81	4.09	3.35	2.70	2.02	1.47
1.3	6.00	4.84	3.78	2.96	2.17	1.55
	7.26	5.83	4.50	3.45	2.44	1.65
	9.07	7.21	5.45	4.03	2.68	1.71
1.4	9.66	7.23	5.20	3.77	2.55	1.69
	12.2	9.09	6.46	4.58	2.96	1.83
	16.4	12.1	8.40	5.69	3.38	1.93
5/3	35.8	20.7	11.3	6.52	3.53	1.98
	45.9	24.4	14.4	8.16	4.24	2.21
	65.6	37.6	20.1	10.9	5.15	2.40
2	166.	66.3	25.2	10.9	4.65	2.24
	184.	74.8	29.1	12.9	5.49	2.50
	217.	90.8	35.6	16.4	6.66	2.76
3	636.	212.	63.8	21.6	6.87	2.66
	637.	213.	64.3	22.2	7.42	2.89
	637.	214.	66.2	24.1	8.39	3.13

TABLE II.

$$k_\eta = k_\eta(\eta_0, \gamma)$$

γ	η_0			
	1	0.3	0.1	0.03
1.1	1	1.22	1.44	1.72
		1.22	1.45	1.73
		1.22	1.45	1.71
1.2	1	1.46	2.03	2.87
		1.47	2.05	2.91
		1.47	2.02	2.70
1.3	1	1.71	2.78	4.74
		1.72	2.81	4.76
		1.71	2.68	4.03
1.4	1	1.95	3.68	7.65
		1.96	3.72	7.52
		1.93	3.38	5.69
5/3	1	2.58	6.53	19.4
		2.56	6.33	17.4
		2.40	5.15	10.9
2	1	3.14	9.07	29.1
		3.04	8.45	25.2
		2.76	6.66	16.4
3	1	3.33	9.99	33.2
		3.32	9.82	31.0
		3.13	8.39	24.1

the time needed to establish the asymptotic expansion regime depends sensitively on the value of the adiabatic index. For γ close to unity the approach to the limiting value is slower. For example, for $\gamma = 1.1$ the value of $k_\zeta(\tau)$ at $\tau = 10^6$ differs by approximately 1% from its limiting value as $\tau \to \infty$.

The data in Tables I and II confirm the conclusion drawn previously, that the expansion of the cloud in the z direction is weakly coupled to its expansion in the (x,y) plane. Nevertheless, these two motions are coupled, and in a certain region of parameter space the interaction can be significant (it may reach tens of percent). This effect can be used to obtain important information about the parameters of the initial vapor cloud. Note the nonmonotonic behavior of the corresponding functions. For example, the ratio of $k_\zeta(\infty)$ at $\eta_0 = 0.1$ to $k_\zeta(\infty)$ at $\eta_0 = 1$ increases as a function of γ for $\gamma < 5/3$ and falls off for $\gamma > 5/3$.

4. TIME-OF-FLIGHT SPECTRA

One of the experimentally determined characteristics of the vapor expansion process is the time dependence of the number density of the evaporated atoms at a fixed point in space. Mass spectroscopy techniques are usually employed to measure this quantity. For this purpose the time-of-flight technique, first used to analyze the products of vaporization induced by a laser pulse more than thirty years ago,[32] proves convenient. In these and similar studies most of the attention is paid to the fast ions, which move in the collisionless regime in the external region of the laser flare. In this case the interpretation of time-of-flight spectra does not give rise to difficulty. Matters become more complicated when we study

the dynamics of a dense cloud expanding in a dense medium. Note that in a number of investigations (cf. Refs. 14, 33, and 34) the results of time-of-flight mass spectrometry of laser flares were interpreted by taking the mass velocity of the vapor flow in the inertial stage to be the same as the thermal velocity of particles in some hypothetical Maxwellian distribution, and the temperature of this distribution was derived from the experimental data. This procedure makes use of a formal analogy between a Maxwellian distribution and the Gaussian density profile in an isothermal gasdynamic flow with uniform deformation. But if the flow is not strictly isothermal (which is always the case), the density profile is not Gaussian and this formal analogy cannot be employed. It is clear that the quantity determined by the above methods does not have the properties of a thermodynamic temperature. This can be seen from the fact that such a "temperature" is different for the distributions of different velocity components, with the differences being dependent on the geometry of the initial vapor cloud (thus, the use of the term "elliptical temperature" in Ref. 14 does not make the procedure in question more rigorous physically).

In actuality, as a function of time particles propagating under different conditions and in different regimes pass through a given observation point. The behavior varies from free molecular motion at the edge of the expanding cloud to a dense medium with a local equilibrium distribution of atoms in the densest part (see, e.g., Ref. 35). A rigorous description of the vapor flow in the general case requires solution of the kinetic equation. The simplest examples of such a solution are given in Refs. 36 and 37, where numerical techniques were used to study plane and spherically symmetric
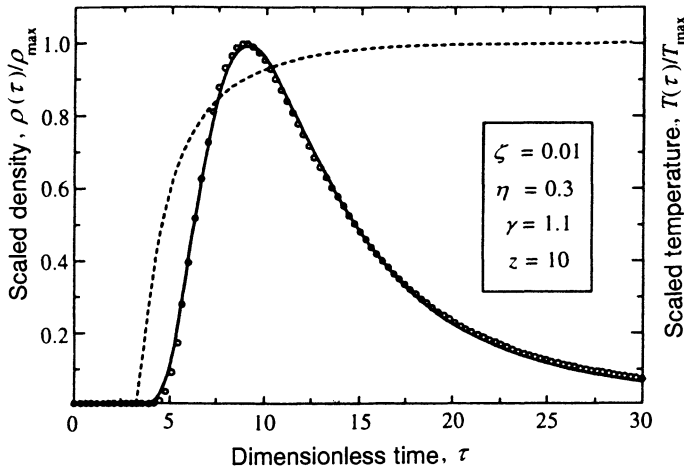
FIG. 4. Time variation of the density (circles) and temperature (broken curve) of the vapor at the point $z = 10$ on the z axis. The solid curve corresponds to the approximate form of $\rho(t)$ given by Eq. (19).

expansion respectively of vapor into a vacuum. In these cases, when the vapor density is high and the hydrodynamic description is valid, it is natural to use the adiabatic solution of the gasdynamic equations discussed in the present work to analyze the results of time-of-flight mass spectrometry. In Fig. 4 the circles indicate the vapor density at an observation point on the z axis ($z = 10$, $\gamma = 1.1$) derived using this solution. It is noteworthy that this dependence is accurately approximated by a Gaussian function,

$$\rho_m(\tau) = \frac{A}{\tau^3} \exp\left[-B\left(\frac{z}{\tau} - u\right)^2 \right], \tag{19}$$

with the constants given by $A = 1801.2$, $B = 2.53667$, and $u = 0.4368$. Expressions of the form (19) were used to describe time-of-flight spectra in Ref. 14. It is clear that the adiabatic solution (10) can be used equally well to analyze experimental data. The only difference is that the parameters that enter into Eq. (10) have a clear physical meaning.

It is of interest to compare the functions (10) and (19) in the inertial stage of the expansion, when

$$X \approx v_x\tau, \quad Y \approx v_y\tau, \quad Z \approx v_z\tau. \tag{20}$$

At points on the z axis the vapor density for $\tau > z/v_z$ is given by

$$\rho(\tau) = \frac{M}{I_1(\gamma) v_x v_y v_z^{(\gamma+1)/(\gamma-1)}} \frac{1}{\tau^3} \left(v_z^2 - \frac{z^2}{\tau^2} \right)^{1/\gamma - 1}, \tag{21}$$

which follows directly from (10) and (20). Both expressions, (19) and (21), have the same asymptotic behavior ($\propto \tau^{-3}$) for large τ. By adjusting the parameters appropriately in Eq. (19) we can approximate the maxima and widths of these distributions closely (this is especially simple when γ is close to unity). However, the vapor temperature determined by solving the gasdynamic equations is of course different from the "temperature" found from the width of the Maxwellian distribution approximating the gasdynamic solution. For the example given in Fig. 4 the time dependence of the vapor pressure at the observation point $z = 10$ is shown by the broken

trace. The temperature reaches a maximum at time $\tau = 26.7$ and then slowly falls off with increasing time. This slow variation is a consequence of the fact that the adiabatic index is close to unity ($\gamma = 1.1$). In an adiabatic process we have

$$T \propto \rho^{\gamma - 1} \propto \rho^{0.1}, \tag{22}$$

i.e., the temperature varies much more slowly than the density. For γ not so close to unity the temperature depends more sensitively on time, and the approximation of the gasdynamic distribution by a function of the form (19) is less accurate.

5. SHAPE OF THE VAPOR CLOUD FOR AN EXPANSION INTO A MEDIUM WITH AN AMBIENT PRESSURE

Equation (9) for the pressure of an adiabatically expanding gas can be used to interpret experimental data on laser ablation in a gaseous medium. In particular, this formula can be used to predict the shape of a vapor cloud expanding into a medium with an ambient pressure.[38,39] As is well known, when vapor expands into a medium with a back-pressure the motion is more complicated than for expansion into a vacuum. A shock wave develops in the surrounding medium. The region containing the gas compressed by the shock is separated from the expanding vapor by a contact discontinuity, which moves with decreasing speed as time increases. Because of the deceleration of the contact discontinuity a second shock wave develops, which propagates into the vapor cloud.

The vapor density near the contact discontinuity is usually higher than that of the gas compressed by the shock wave. This can be traced back to the fact that the pressure on both sides of the contact surface is the same, but the temperature of the gas compressed by the shock is higher than that of the adiabatically expanding vapor. In this situation the contact surface is unstable. An instability of this type is well known in hydrodynamics and is called the Rayleigh–Taylor instability. The nonlinear growth of the instability at the contact surface gives rise to turbulent mixing of the vapor with the surrounding gas near the contact surface. This interaction between the expanding vapor cloud and the gaseous medium is completely analogous to the expansion of the detonation products of a chemical explosive material into the surrounding gas. The associated Taylor instability and turbulent mixing have been studied theoretically,[40,41] and then observed experimentally in Refs. 42 and 43 (for an explosion) and in Refs. 44, 45, and 38 (laser ablation). The shock wave predicted in the calculations of Refs. 41 and 43, which arises in the detonation products due to deceleration of the contact surface, has also been observed in laser ablation experiments.[21]

The laser flare model discussed in the present work enables us to study the effect of the pressure of the surrounding gas on the dynamics of the motion of the contact surface for small values of the gas pressure. In this case we can assume that the contact surface is described by
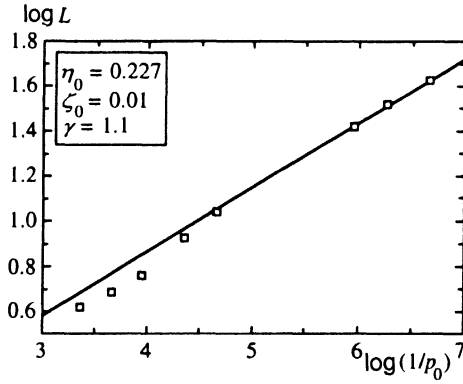
$$p(x,y,z,t) = P_0 \tag{23}$$

FIG. 5. Size of the stationary cloud as a function of the pressure of a surrounding gas.

where the vapor pressure $p(x,y,z,t)$ is given by Eq. (9) and P_0 is the pressure of the surrounding gaseous medium. In dimensionless form this equation becomes

$$p_0 = \frac{1}{I_2(\gamma)} (\xi\eta\zeta)^{-\gamma} \left[1 - \frac{\tilde{x}^2}{\xi^2} - \frac{\tilde{y}^2}{\eta^2} - \frac{\tilde{z}^2}{\zeta^2} \right]^{\gamma/\gamma - 1} \quad (24)$$

where the dimensionless quantities p_0, $\tilde{x}$, $\tilde{y}$, $\tilde{z}$ are given by

$$p_0 = \frac{P_0 X_0^3}{E}, \quad \tilde{x} = \frac{x}{X_0}, \quad \tilde{y} = \frac{y}{Y_0}, \quad \tilde{z} = \frac{z}{Z_0}. \quad (25)$$

At each point $(\tilde{x},\tilde{y},\tilde{z})$ of the surface defined by Eq. (24) the distance from the coordinate origin reaches a maximum value at some time $\tau = \tau^*(\tilde{x},\tilde{y},\tilde{z})$. At that point in time the group velocity vanishes. The set of all stopping points of the contact surface forms the boundary of the so-called steady vapor cloud. With sufficiently rapid exposure times the position of this boundary can readily be detected experimentally by means of photography.[38,39] The length L of the stationary cloud in the z direction is given by

$$L = \{1 - [\xi(\tau^*)\eta(\tau^*)\zeta(\tau^*)]^{(\gamma-1)}$$

$$\times [p_0 I_2(\gamma)]^{\gamma - 1/\gamma}\}^{1/2}\zeta(\tau^*)X_0. \quad (26)$$

An example of this behavior together with experimental data[38] is shown in Fig. 5. In the experiments of Ref. 38 ablation of a high-temperature superconducting $YBa_2Cu_3O_7$ ceramic was studied in an O_2 atmosphere, under the action of a KrF excimer laser. For these data the pulse energy was always equal to 100 mJ, and the dimensions of the focal spot were $X_0 = 1.1$ mm, $Y_0 = 0.25$ mm. In dimensional units the experimental point at the upper right in Fig. 5 corresponds to an oxygen pressure $P_0 = 0.2$ mbar and a stationary cloud length $z_l = 43$ mm. As can be seen from the figure, the results of the corresponding calculations are in good agreement with experiment.

One property of this model is that it predicts a power-law dependence of the cloud length L on the gas pressure P_0 over a broad range of parameters:

$$L \approx G p_0^{-\beta}. \quad (27)$$

The constants G and β are easily found analytically for the case of a spherical expansion (see Ref. 38):

TABLE III.

$$\beta = \beta(\zeta_0, \gamma)$$

γ	ζ_0		
	0.01	0.03	1
1.1	0.281	0.284	0.303
	0.286	0.288	0.307
1.2	0.264	0.266	0.278
	0.268	0.270	0.280

$$G = \sqrt{3(\gamma-1)} 2^{1/3(\gamma-1)}(3\gamma-1)^{1-3\gamma/6(\gamma-1)} I_2(\gamma)^{-1/3\gamma}, \quad (28)$$

$$\beta = \frac{1}{3\gamma}. \quad (29)$$

In the case of an ellipsoidal vapor cloud these coefficients also depend on the values of η_0 and ζ_0. The dependence of the exponent β on η_0, ζ_0, and γ can be found by calculating L numerically from Eq. (26). An idea of this dependence can be gotten from Table III. In each box of the table two values of β are given, for $\eta_0 = 1$ (upper row) and $\eta_0 = 0.3$. It is clear that β depends weakly on the parameters, so in order to estimate the adiabatic index from the measured value of the flare length as a function of pressure in the surrounding medium we can use Eq. (29). The experiments recently carried out by Proyer et al.[39] confirm that a dependence of the form (27) actually occurs over a wide range of variation of the pressure P_0. The departure from this behavior at high pressures (for the experimental data used in Fig. 5, at $P_0 > 400$ mbar) is related to the development of the Taylor instability, while that at low pressures is associated with the finite lifetime of the excited molecules which are responsible for the photographic image of the vapor cloud (for more details see Ref. 39). Because the power-law dependence persists over a broad range of pressures (approximately three orders of magnitude of variation in P_0), the exponent β can be reliably determined. Such measurements make it possible to develop a diagnostic for the vaporized material. In particular, by comparing the calculated and experimental data in Fig. 5 we can find the value $\beta = 0.287$ for the exponent. This yields $\gamma \approx 1.16$, which agrees well with the values $1.1 \leq \gamma \leq 1.3$ given in Refs. 34 and 46, and is typical for laser ablation of high-temperature superconducting ceramics.

6. PROFILE OF THE FILM THICKNESS

The solution obtained above enables us to calculate the profile of the film thickness deposited from a vapor cloud expanding onto a planar substrate. We will assume that the plane of the substrate is perpendicular to the z axis and located at a distance z_s from the evaporated target (Fig. 1). The mass flux density onto the substrate can be expressed in the form

$$j(x,y,z_s,t) = \rho(x,y,z_s,t)v_z(x,y,z_s,t)$$

$$= \begin{cases} \dfrac{M z_s \dot{Z}}{I_1(\gamma) XYZ^2} \left[1 - \dfrac{x^2}{X^2} - \dfrac{y^2}{Y^2} - \dfrac{z^2}{Z^2} \right]^{-1/(\gamma-1)} , & t \geqslant t_s(x,y), \\ 0, & t < t_s(x,y). \end{cases}$$

$$(30)$$

Here $t_s(x,y)$ is the time at which the exterior boundary of the expanding cloud reaches the substrate $(z=z_s)$ at the point (x,y). This time can be found by solving the equation

$$\frac{x^2}{X^2(t_s)} + \frac{y^2}{Y^2(t_s)} + \frac{z_s^2}{Z^2(t_s)} = 1. \tag{31}$$

By integrating the mass flux (30) with respect to time and dividing the result by the film density ρ_s we find the profile of the thickness in the form

$$h(\theta_x,\theta_y) = \frac{M z_s}{\rho_s I_1(\gamma)} \int_{t_s}^{\infty} \frac{\dot{Z} dt}{XYZ^2}$$

$$\times \left\{ 1 - z_s^2 \left[\frac{\tan^2 \theta_x}{X^2} + \frac{\tan^2 \theta_y}{Y^2} + \frac{1}{Z^2} \right] \right\}^{1/(\gamma-1)},$$

$$(32)$$

where

$$\tan \theta_x = \frac{x}{z_s}, \quad \tan \theta_y = \frac{y}{z_s}. \tag{33}$$

In the general case the integration in (32) can be performed only by numerical means and by using the functions $X(t)$, $Y(t)$, and $Z(t)$ obtained by numerical solution of Eq. (15). However, in experiments on laser film deposition the inequality $z_s \gg X_0$ often holds. In this limit the integral (32) can be evaluated analytically and yields a simple formula for the profile of the film thickness. Specifically, this inequality is equivalent to $t_s \gg X_0/\beta^{1/2}$, which means that the expanding cloud reaches the substrate in the inertial stage of the expansion. Then the lengths of the axes of the ellipsoid are related linearly:

$$X(t) = Z(t)/k_\zeta(\infty) \quad \text{and} \quad Y(t) = Z(t) k_\eta(\infty)/k_\zeta(\infty). \tag{34}$$

Substituting (34) in (32) and using (31) we find the profile of the thickness in the form

$$h(\theta_x,\theta_y) = \frac{Mpq^2}{2\pi\rho_s z_s^2} [p + \tan^2 \theta_x + q^2 \tan^2 \theta_y]^{-3/2}, \tag{35}$$

where $p = 1/k_\zeta(\infty)$ and $q = 1/k_\eta(\infty)$.

In the analysis of experimental data the assumption is often made that

$$h(\theta_x,\theta_y) \propto \cos^m \theta_x \cos^n \theta_y. \tag{36}$$

The formula (35) which we have derived departs from this approximation. But at small angles $\theta_x \ll \arctan p$, $\theta_y \ll \arctan q$ the two profiles are identical under the conditions

$$m = 3k_\zeta^2, \quad n = 3k_\zeta^2/k_\eta^2. \tag{37}$$

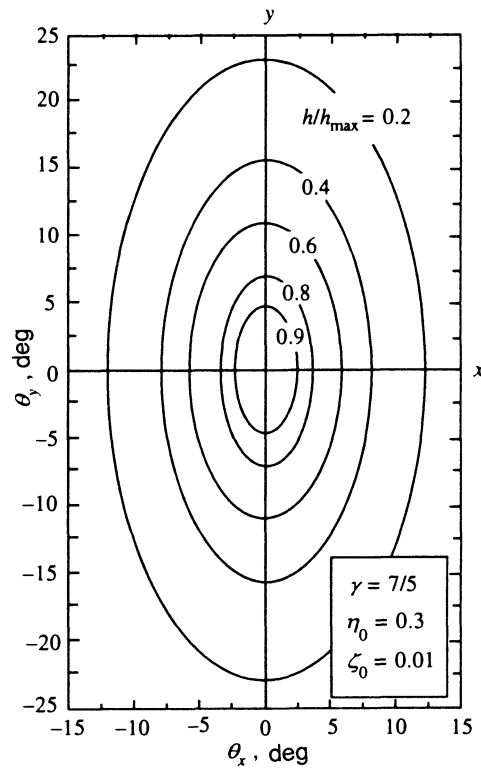In the special case of spherical expansion (35) yields the relation

FIG. 6. Profile of the film thickness. Shown are contours of constant density calculated from Eq. (35).

$$h(\theta) = \frac{M}{2\pi\rho_s z_s^2} \cos^3 \theta. \tag{38}$$

Here θ is the polar angle in a spherical coordinate system. The formula (38) can easily be derived directly from the mass conservation condition.

A contour plot of the function $h(\theta_x,\theta_y)$ derived from Eq. (35) is shown in Fig. 6. Comparison with experiment reveals that the formula (35) provides a good description of the thickness profiles for small angles θ_x and θ_y, but at the edges of the spot the film thickness falls off more rapidly than predicted by Eq. (35). One reason for the discrepancy is failure to take into account the dependence of the attachment coefficient on the angle of incidence and the kinetic energy of particles incident on the substrate (see, e.g., Ref. 47). In some cases the asymptotic nature of Eq. (35) may also play a role. Note that the profile of the film thickness can easily be found, even for an arbitrary relation between z_s and X_0. For this it is necessary to perform a simple numerical integration in Eq. (28).

7. CONCLUSION

The relatively simple model considered in the present work provides an opportunity to estimate how the shape of the focal spot affects the spatial structure of the vapor flow in the profile of the film thickness formed when the vapor condenses on a substrate without performing complicated three-dimensional gasdynamic calculations.

The model contains two very important simplifications. First, it is assumed that the initial vapor cloud formed when

the laser pulse acts on the target has an ellipsoidal shape. The exact shape of the cloud is usually not known. A triaxial ellipsoid is a reasonable approximation to the actual shape. By solving the problem of the expansion of this ellipsoid we can establish the basic motion of the vapor, namely, that the expansion of a nonspherical cloud proceeds fastest in the direction of its shortest axis. Thus we have explained the flipover effect.

The second important simplification in the problem is that we have assumed the specific entropy to be constant through the interior of the cloud. No reliable information is available about the entropy distribution in an actual cloud. There are indications that the expanding cloud of laser ablation products is nonisothermal.[19,29] The isothermal models considered in Refs. 10, 11, and 14 are therefore far from reality. At the same time, the question of the entropy profile in an expanding gas cloud assumes particular interest in connection with the convective instability of the cloud described in Ref. 48 for the case in which the entropy in the external layers of gas is less than that in the internal layers (see also Ref. 49). Although the analysis of Ref. 48 applies only to a spherically symmetric cloud, simple qualitative arguments suggest that the expansion of an ellipsoidal cloud under similar conditions can also be unstable. As far as we know, this type of instability in the expansion of vapor into vacuum has not yet been observed in laser ablation experiments. Consequently, if the initial cloud does have a significant entropy gradient, then it cannot be directed toward the center of the cloud. Of course the model of an isentropic cloud we have constructed cannot be used to describe such an instability.

The particular solution of the gasdynamic equations considered above can be used to interpret the results of time-of-flight mass spectrometry. We emphasize that the width of the particle distribution as a function of the time of flight (which depends on the observation angle) cannot be interpreted as the vapor temperature.

Another way to use this solution of the gasdynamic equations is connected with the study of the effect of the pressure of the surrounding gas on the shape of the expanding vapor cloud. The results of the corresponding calculations (see Fig. 5) when the gas pressure is low are in good agreement with experiment.[38,39]

In the range of parameters typical of the laser technique for depositing thin films the profile of the film thickness can be described by a simple analytical formula (35). This formula implies that at small angles θ_x and θ_y the film thickness is proportional to $\cos^m\theta_x\cos^n\theta_y$, where the exponents m and n are determined by the asymptotic behavior of the expanding cloud [cf. Eq. (37) and Tables I and II]. For typical experimental conditions the calculation yields values of m and n in the range from a few times unity to several times ten, which agrees with the experimental results. Since the shape of the focal spot can easily be controlled in the experiments, the analysis described above permits important information about the parameters of the initial vapor cloud to be derived from exact measurements of the exponents m and n in the distribution of the film thickness.

[1] S. V. Gaponov, Usp. Fiz. Nauk 146, 343 (1985) [Sov. Phys. Usp. 28, 522 (1985)].

[2] D. Bauerle, Appl. Phys. A 48, 527 (1989).

[3] É. N. Sobol', V. N. Bagratashvili et al., "Review of high-temperature superconductivity," in Handbook of the International Center for Scientific and Technical Information No. 3, Moscow (1990).

[4] E. Fogarassy and S. Lasare (eds.), "Laser ablation of electronic materials. Basic mechanisms and applications," Proc. E-MRS 4, North Holland (1993).

[5] L. D. Laude (ed.), "Excimer lasers," NATO ASI Series, E256, Kluwer Academic Publishers, Dordrecht (1994).

[6] D. Bauerle, E. Arenholz et al., in Material Science Forum Vols. 173–174, 41 (1995).

[7] A. D. Aksakhalyan, S. V. Gaponov et al., Zh. Tekh. Fiz. 58, 1885 (1988) [Sov. Phys. Tech. Phys. 33, 1146 (1988)].

[8] T. Venkatesan, X. D. Wu et al., Appl. Phys. Lett. 52, 1193 (1988).

[9] R. K. Singh, N. Biuno, and J. Narayan, Appl. Phys. Lett. 53, 1013 (1988).

[10] R. K. Singh and J. Narayan, Phys. Rev. B 41, 8843 (1990).

[11] R. K. Singh, O. W. Holland, and J. Narayan, J. Appl. Phys. 68, 233 (1990).

[12] C. N. Afonso, R. Serna et al., Appl. Surf. Sci. 46, 249 (1990).

[13] R. E. Muenchausen, K. N. Hubbard et al., Appl. Phys. Lett. 56, 578 (1990).

[14] J. C. L. Kools, T. S. Baller et al., J. Appl. Phys. 68, 233 (1992).

[15] A. Miotello, R. Kelly et al., Appl. Phys. Lett. 61, 2784 (1992).

[16] F. Davanloo, E. M. Juengerman et al., Appl. Phys. A 54, 369 (1992).

[17] S. I. Anisimov, D. Baeuerle, and B. S. Luk'yanchuk, Phys. Rev. B 48, 12076 (1993).

[18] R. Kelly and A. Miotello, Nucl. Instrum. and Methods in Phys. Res. B 91, 82 (1994).

[19] N. G. Basov, V. A. Boiko et al., Zh. Éksp. Teor. Fiz. 51, 969 (1966) [Sov. Phys. JETP 24, 659 (1967)].

[20] A. D. Aksakhalyan, Yu. A. Bityurin et al., Preprint, Inst. Appl. Phys. Acad. Sci. USSR, Gor'kii (1981).

[21] D. B. Geohegan, Thin Solid Films 220, 138 (1992).

[22] M. K. Matzen and R. L. Morse, Phys. Fluids 22, 654 (1979).

[23] L. V. Ovsyannikov, Group Analysis of Differential Equations, Academic, New York (1982).

[24] L. V. Ovsyannikov, Lectures in Basic Gasdynamics, [in Russian], Nauka, Moscow (1981).

[25] L. I. Sedov, Dokl. Akad. Nauk SSSR 90, 735 (1953).

[26] L. V. Ovsyannikov, Dokl. Akad. Nauk SSSR 111, 47 (1956).

[27] F. J. Dyson, J. Math. Mech. 18, 91 (1968).

[28] J. M. Dawson, P. Kaw, and B. Green, Phys. Fluids 12, 875.

[29] I. V. Nemchinov, Prikl. Mat. Mekh. 29, (1965).

[30] S. I. Anisimov and Yu. I. Lysikov, Prikl. Mat. Mekh. 34, 926 (1970).

[31] O. I. Bogoyavlenskiĭ, Methods for the Qualitative Treatment of Dynamical Systems in Astrophysics and Gasdynamics, [in Russian], Nauka, Moscow (1980).

[32] N. R. Isenor, Appl. Phys. Lett. 4, 152 (1964).

[33] J. P. Zheng, Q. Y. Ying et al., Appl. Phys. Lett. 54, 954 (1989).

[34] N. H. Cheung, Q. Y. Ying et al., J. Appl. Phys. 69, 6349 (1991).

[35] R. Kelly and R. W. Dreyfus, Nucl. Instrum. and Methods in Phys. Res. B 32, 341 (1988).

[36] S. I. Anisimov and A. Kh. Rakhmatulina, Zh. Éksp. Teor. Fiz. 64, 869 (1973) [Sov. Phys. JETP 37, 441 (1973)].

[37] V. I. Zhuk, Izv. Akad. Nauk SSSR, Mekh. Zhid. Gazov, No. 2, 97 (1976).

[38] E. Stangl, B. Luk'yanchuk et al., in L. D. Laude (Ed.), Excimer Lasers, Kluwer Academic Dordrecht (1994).

[39] S. Proyer, E. Stangl, and D. Baeuerle, Appl. Phys. A (1995) (in press).

[40] S. I. Anisimov and Ya. B. Zel'dovich, Pis'ma Zh. Tekh. Fiz. 3, 1081 (1977) [Sov. Tech. Phys. Lett. 3, 645 (1977)].

[41] S. I. Anisimov, Ya. B. Zeldovich, N. A. Inogamov, and M. F. Ivanov, in *Shock Waves, Explosions and Detonations*, AIAA Prog. in Astron. and Aeron. Series, Vol. 87, p. 218 (1983).

[42] A. N. Davydov, E. F. Lebedev, and A. V. Shurupov, Pis'ma Zh. Tekh. Fiz. **9**, 429 (1983) [Sov. Tech. Phys. Lett. **9**, 185 (1983)].

[43] A. V. Shurupov, A. N. Davydov *et al.*, "Cylindrical Explosive Flows," Preprint No. 2-157, High-Temperature Inst., AN SSSR, Moscow (1985).

[44] K. Scott, J. M. Hantley *et al.*, Appl. Phys. Lett. **57**, 922 (1990).

[45] R. Srinivassan, Appl. Phys. A **56**, 417 (1993).

[46] R. Kelly and A. Miotello, Appl. Phys. B **57**, 145 (1993).

[47] B. McCarrol and G. Ehrlich, J. Chem. Phys. **38**, 523 (1963).

[48] D. L. Book, J. Fluid Mech. **95**, 779 (1979).

[49] L. D. Landau and E. M. Lifschitz, *Fluid Mechanics*, Pergamon, Oxford (1984).

Translated by David L. Book